Journal of Solid State Chemistry 183 (2010) 1063–1070

Contents lists available at ScienceDirect

Journal of Solid State Chemistry

journal homepage: www.elsevier.com/locate/jssc

Estimation of the intrinsic stresses in α-alumina in relation with its elaboration mode

A. Boumaza *, A. Djelloul

Laboratoire des Structures, Propriétés et Interactions Inter Atomiques (LASPI2A), Center Universitaire de Khenchela, Khenchela 40000, Algeria

ARTICLE INFO

Article history:
Received 18 April 2009
Received in revised form
21 January 2010
Accepted 6 March 2010
Available online 12 March 2010

Keywords:
Alpha alumina
Boehmite
Gibbsite
PM2000 alloy
Infrared spectroscopy
X-ray diffraction
Cathodoluminescence
Oxygen vacancies

ABSTRACT

The specific signatures of α-Al_2O_3 by Fourier transform infrared (FTIR) spectroscopy were investigated to estimate the intrinsic stress in this compound according to its elaboration mode. Thus, α-alumina was prepared either by calcination of boehmite or gibbsite and also generated by oxidation of a metallic FeCrAl alloy. FTIR results were mainly supported by X-ray diffraction (XRD) patterns that allowed to determine the crystallite size and the strain in the various alpha aluminas. Moreover, the infrared peak at 378.7 cm^{-1} was used as a reference for stress free α-alumina and the shift of this peak allowed to estimate intrinsic stresses, which were related to the morphology and to the specific surface area of aluminas according to their elaboration mode. These interpretations were confirmed by results obtained by cathodoluminescence experiments.

1. Introduction

Most of metallic materials functioning at high temperature need to have oxidation resistance. This resistance can be achieved when the material develops, through oxidation, an oxide film which acts as a diffusion barrier while keeping a good adherence. In this respect, alpha alumina clearly acts as such. In previous studies, TEM was used to probe the oxidation of either an intermetallic alloy, Fe_3Al, or an oxide dispersion strengthening (ODS) FeCrAl alloy strengthened by very small yttria particles, PM2000 [1,2]. It is worth noting, however, that this technique is not generally adapted for probing such material. The present study aims at investigating whether the FTIR spectroscopy may provide signatures of α-Al_2O_3 taking into account the intrinsic stress level in the material as stresses should induce a shift of the peak position. Amongst all origins of stresses, defects due to non-stoichiometry should act on their infrared peaks position [3–5].

In the case of films, it is generally accepted that the overall stress of a thin film is given by a sum of the intrinsic stress, the growth stress and the thermal stress components. The intrinsic stress component is residual internal stress after eliminating or accounting for the growth stress and the thermally induced stresses. This is obtained by scraping the film. Furthermore, intrinsic stresses are attributed to the incorporation of excess vacancies and to the presence of interstitials and similar defects.

The aim of this paper is to bring a contribution in this field, based on some of our experimental results previously obtained on α-alumina by X-ray diffraction (XRD) and Fourier transform infrared spectroscopy (FTIR) which allowed to characterize transition and α-alumina structures [6]. In this paper, we investigated the specific signatures of α-Al_2O_3 by FTIR spectroscopy in order to estimate the intrinsic stress in this compound according to its elaboration mode. Thus, α-alumina was prepared either by calcination of boehmite or gibbsite and also generated by oxidation of a metallic alloy. Thus, this manuscript correlates the microstrain, determined from X-ray measurements, with the stresses determined with infrared spectroscopy and supported by cathodoluminiscence experiments.

2. Experimental procedure

Dispal 21N4–80 boehmite powder, AlOOH, from Vista and gibbsite powder, $Al_2(OH)_6$, from Prolabo (no. 20984) were used. The boehmite powder and gibbsite platelets were calcined in ambient atmosphere ($pO_2 = 0.21$ atm) at 1573 K. The cycle was as follows:

- heating up to an isothermal temperature at 5 K/min,

* Corresponding author. Fax: +21332331960.
E-mail addresses: charif_boumaza@yahoo.com (A. Boumaza), djelloulabdelkader@yahoo.fr (A. Djelloul).

0022-4596/$ - see front matter © 2010 Elsevier Inc. All rights reserved.
doi:10.1016/j.jssc.2010.03.012

- maintaining for 24 h at the calcination temperature,
- fast cooling down to room temperature (air quench).

The calcination temperature was maintained for 24 h to obtain a well-crystallised product. After calcination, 10 to 100 μg of the powder was drawn, then grinded with 23 ± 2 mg of CsBr in order to obtain a pellet of 200–250 μm in thickness. After grinding, the powder was placed in a mould (5 mm diameter) and a cold isostatic pressure (CIP) of 150 MPa was applied for 5 min.

In the case of the PM2000 FeCrAl ODS alloy, samples were oxidized in air at temperatures ranging between 1023 and 1223 K. For the FTIR measurements, samples were prepared by grinding the oxide films scraped from the substrate.

The FTIR technique was used in the absorbance mode in the 200–4000 cm^{-1} range. For oxides all bands have characteristic frequencies between 200 and 1000 cm^{-1}.The FTIR spectra are obtained using a Perkin-Elmer spectrometer at resolution of 8 cm^{-1}. For each sample, 120 scans were used. The apparatus is equipped with a system allowing the reduction of the optical course in air in order to minimize the perturbations associated with ambient air (water vapour and CO_2). The uncertainty on the position of the various peaks is equal to ± 2 cm^{-1}.

The crystalline structure of the calcined powders and of the oxidized PM2000 was investigated by XRD using a PANalytical X'Pert Pro MRD diffractometer configured as follows: Cu tube operating at 40 kV and 30 mA (weighted mean wavelength = 0.15406 nm), the diffraction data were collected over a 2θ range 10–80°, with a step width of 0.025°.

The thermogravimetric method (TG) and differential thermal analysis (DTA) data were recorded under a dry air flow with a heating rate of 10 K/min in a SETARAM TGDTA92-16.18 thermal analyser. TG measurements were corrected for temperature-dependent buoyancy by subtracting the data of a measurement carried out on an inert sample.

The emitted light under electron beam excitation in a UHV system was analyzed through a quartz window with a Jobin Yvon CP 2000 spectrograph and a CCD detector. The wavelength range 200–1000 nm was investigated. The cathodoluminescence (CL) spectra were recorded in a computer.

3. Results

The boehmite powder is made of spherical aggregates whose diameter ranges from 3 to 50 μm, as shown in Fig. 1A. In Fig. 1C (curve (a)), the XRD pattern obtained on the as-received boehmite powder shows a good agreement with the reference XRD pattern (21-1307 JCPDS file). Gibbsite powder is made of platelet aggregates as shown in Fig. 2A. In Fig. 2C (curve (a′)) the XRD pattern obtained on the as-received gibbsite powder shows a good agreement with the reference XRD pattern (33-0018 JCPDS file).

Typical TG–DTA curves of the boehmite are reported in Fig. 3a. The dehydration–dehydroxylation appears to occur in three main steps which will be described and discussed further on.

For gibbsite (Fig. 3b), the dehydration appears to occur in two steps (around 598 and 803 K, respectively) at higher temperature.

Figs. 1 and 2 give SEM images, XRD patterns and FTIR spectra of α-Al_2O_3 obtained by calcination of boehmite or gibbsite, compared to the same data obtained on the initial compound.

In Fig. 4, similar results are given for the PM2000 after oxidation at 1023 K for 76 h and 1223 K for 72 h. The XRD patterns of the α-Al_2O_3 (Fig. 1C (curve (b)), Fig. 2C (curve (b′)) and Fig. 4C (curve at the top)) shows good agreement with the reference XRD α-Al_2O_3 pattern (46-1212 JCPDS file).

Information on the crystallite size and strain for the α-Al_2O_3 was obtained from the full-width at half-maximum of the diffraction peaks. In a first approximation, the full-width at half-maximum β can be expressed as a linear combination of the contributions from the particle size, D, and strain, ε, through the relation [7]

$$\frac{\beta\cos(\theta)}{\lambda} = \frac{1}{D} + \frac{4\varepsilon\sin(\theta)}{\lambda}, \quad (1)$$

with λ the X-ray wavelength (0.15406 nm) and θ the Bragg diffraction angle. The values of β and θ parameters are estimated by Gaussian fitting of the XRD peaks. This formula is not limited by the preferential orientation and is valid for an ordinary XRD profile. In order to improve the statistics, the (0 1 2), (1 0 4), (1 1 3), (0 2 4) and (1 1 6) diffractions peaks of α-Al_2O_3 were chosen to calculate the strain and crystallite sizes since they are prominent in the involved profiles. The plot of $\beta\cos(\theta)/\lambda$ versus $4\sin(\theta)/\lambda$ allows us to determine both the strain and the crystallite size from the slope and the intercept of the curve with the origin of the graph. The estimated values for different α-Al_2O_3 obtained after calcination of gibbsite, boehmite or oxidation of PM2000 are listed in Table 1.

Figs. 5b and d show EDX analyses of the films obtained after oxidation of PM2000 at 1023 K, 76 h (top) and 1123 K, 95 h (bottom).

Cathodoluminescence (CL) signal is a good signature of the material qualities and is used in this study to characterize the point defects associated to oxygen vacancies in α-Al_2O_3 powder. The CL spectra of α-Al_2O_3 formed from boehmite, gibbsite and PM2000 are given in Figs. 6–8.

4. Discussion

4.1. Characterization

Concerning the dehydration–dehydroxylation process of boehmite (Fig. 3a), three steps can be observed. The first step (297–473 K) gives a sharp symmetrical endotherm. It accounts for 5–6% of the mass loss which corresponds to the dehydration of physisorbed water molecules and of part of the chemisorbed molecules. The second step (473–773 K) gives a broad endotherm. It represents the major part of the mass loss (about 15%) which is due to the removal of chemisorbed molecules and to the decomposition of boehmite into γ-alumina [8]. The last step (773–1273 K) gives no thermal event but appears as a continuous mass loss (about 2%) which corresponds to the elimination of residual hydroxyls. The exotherm, which appears at 1468–1508 K of DTA curve, corresponds to the transformation into α-alumina [9]. For a dry boehmite and without nitrate the theoretical mass loss is 15%. Here, the experimental loss reached 22.5%. The initial loss is likely to correspond to water weakly bound. We also note that the dehydration is complete at more than 1273 K; the transition alumina (gamma/delta) most likely contains OH groups.

For gibbsite (Fig. 3b), the expected theoretical loss due to dehydration is 34.6%, the experimental loss is 34.3% a little lower. This difference 0.3% is a bit larger than the experimental uncertainty 0.1%, the starting gibbsite may be slightly dehydrated. The formation of alpha alumina occurs between 1473 and 1533 K [10], it is softer than in the case of boehmite.

As shown by results in Table 1, all the samples were of nearly equivalent average crystallite size (31–43 nm); nevertheless, the crystallite size increases as it follows: "boehmite < PM 2000 < gibbsite".

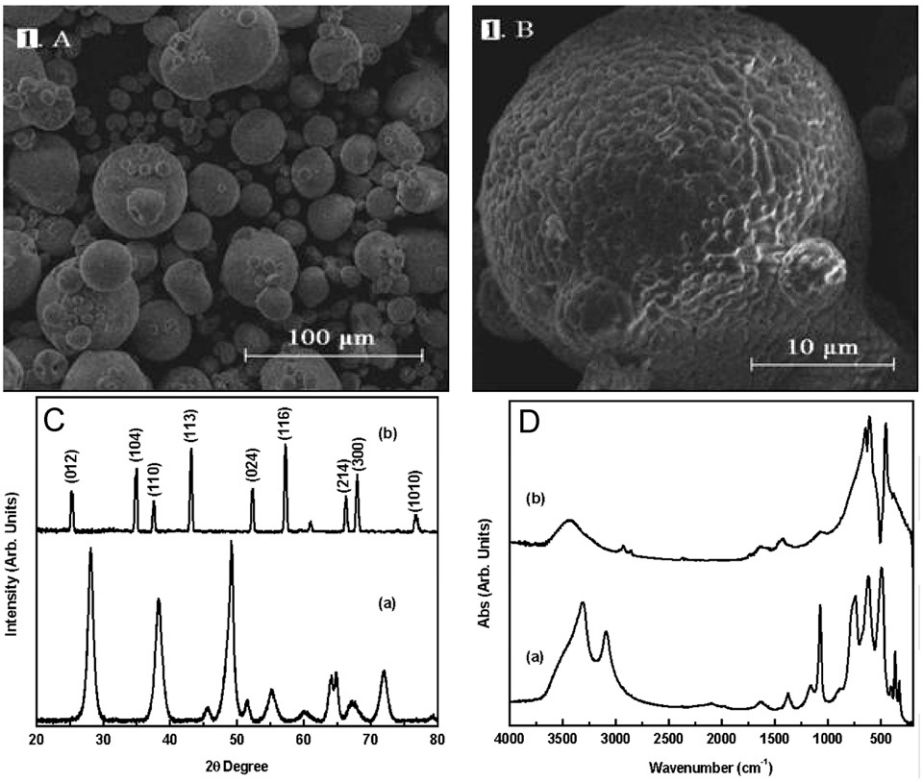

Fig. 1. SEM images (A,B), XRD patterns (C) and FTIR spectra (D) of α-Al_2O_3 powder (curves (b)) obtained by calcination at 1573 K for 24 h of boehmite powder (curves (a)).

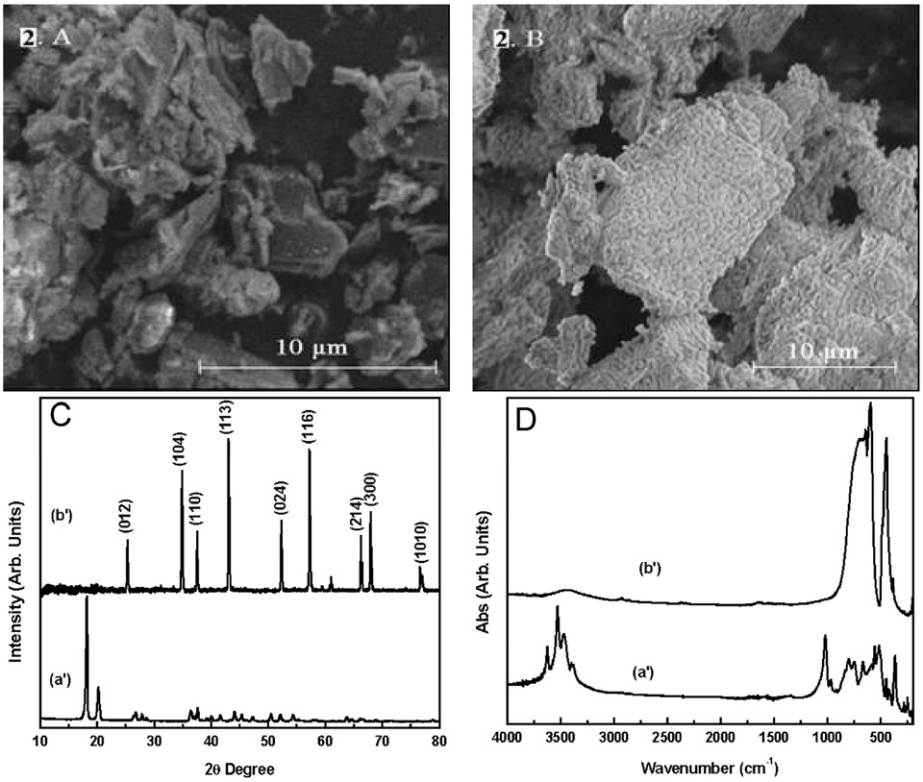

Fig. 2. SEM images (A,B), XRD patterns (C) and FTIR spectra (D) of α-Al_2O_3 powders (curves (b′)) obtained by calcination at 1573 K for 24 h of gibbsite powder (curves (a′)).

The mean crystallite sizes are, in all cases, substantially smaller than the dimension of grains observed in SEM images, indicating that these grains consist in aggregates of many crystallites.

From the strain values (ε), increasing as "boehmite < gibbsite < PM 2000", it is possible to estimate the stress in alumina using, in a first approximation, an elastic model [7] ($|\sigma| = E\varepsilon/\nu$ for alumina

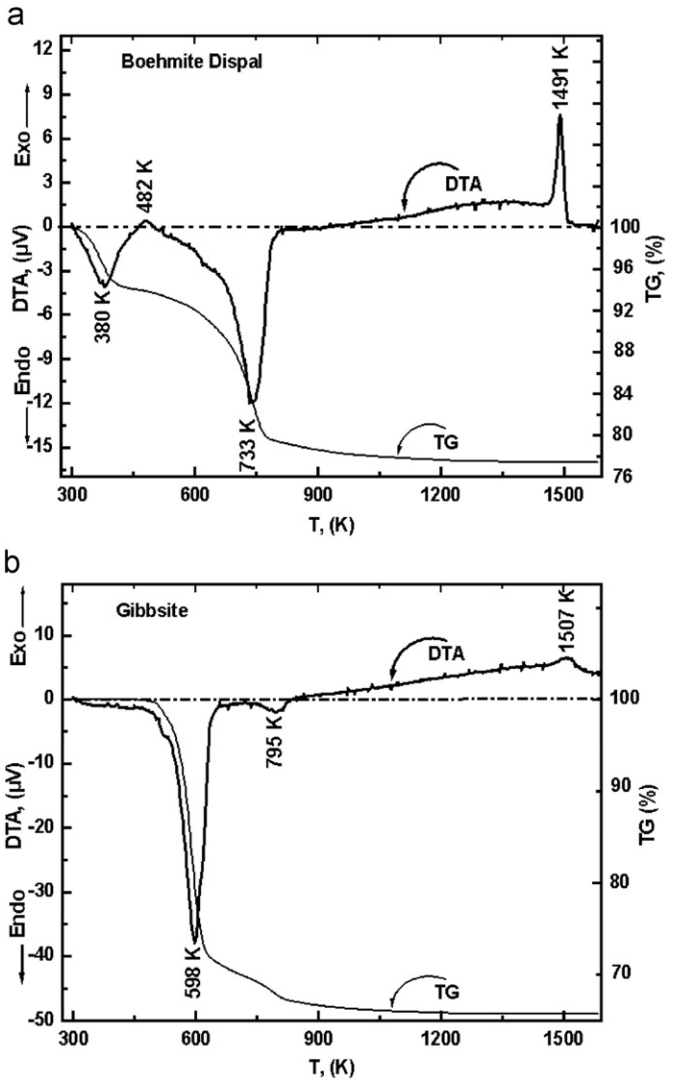

Fig. 3. TG and DTA curves of Boehmite (a) and gibbsite (b).

powder and $|\sigma|=E\varepsilon/(1-\nu)$ for alumina thin films) and taking the values $E=380$ GPa and $\nu=0.25$ for the alumina Young modulus and Poisson coefficient, respectively. Absolute values of the stress deduced from XRD experiments are also given in Table 1. It clearly appears that the strain and stress in alumina developed by oxidation of PM2000 is much greater than that estimated for boehmite, however it is close to that found for gibbsite. This is very satisfying as it has long been recognized that significant stress levels, which are in most cases compressive, can develop in scales as a result of alumina growth. The classic model of Pilling and Bedworth explains for a part the stresses induced by oxide growth [11]. In this model, compressive stresses are related to an increase in volume, as the metal is converted into oxide. The PBR (Pilling–Bedworth ratio) can be calculated using the following equation:

$$\mathrm{PBR}=\frac{\rho_M M_{M_xO_y}}{x\, m_M \rho_{M_xO_y}}, \tag{2}$$

where M_{MO} is the molecular mass of the oxide, m_M the atomic mass of the metal, ρ_{MO} the volumic mass of the oxide, ρ_M the volumic mass of the metal and x the number of oxygen per metal atom. Compressive stresses are developed in the oxide when PBR >1, which is the case here as the PBR for Al/Al_2O_3 is equal to 1.28. Moreover, during cooling of the system from the oxidation temperature, due to the difference between the expansion coefficient of the metallic substrate and that of the oxide film, compressive strains are also generated [12]. As a consequence of these two phenomena which are specific to oxide films, compressive stresses are present in the Al_2O_3 films formed on PM2000.

The specific surface areas (S_{ssa}) of the α-Al_2O_3 crystallites were calculated on the basis of the correlation between the surface area and the crystallite size as follows [13]:

$$S_{ssa}=\frac{6}{\rho_\alpha D}, \tag{3}$$

where D is the average crystallite size and ρ_α is the volumic mass of α-Al_2O_3 ($\rho_\alpha=3.99\,g/cm^3$) [14]. The calcined boehmite sample has a specific surface area of 48 m^2/g, Table 1, much higher than that of the calcined gibbsite (35 m^2/g) and of alumina formed by oxidation of PM2000 samples (42 m^2/g). The increasing sequence is as follows: "gibbsite < PM 2000 < boehmite".

EDX analysis (Fig. 5) of the sample oxidized at 1123 K indicates that the film mainly consists in aluminium and oxygen elements and very small amount of the substrate constituting elements are observed. As the film thickness decreases, like sample oxidized at 1023 K, the signature of the substrate increases due to interactions of the electrons with the underlying substrate mater as the film is thinner than that formed at 1123 K.

4.2. Estimation of intrinsic stress in α-Al_2O_3

The FTIR absorption spectra of alpha alumina obtained from calcination of boehmite, gibbsite and oxidation of PM2000 are shown in Figs. 1D, 2D and 4D. The presence of a strong absorbance band between 3200 and 3600 cm^{-1} is considered to be arising from the associated hydroxyl groups [15]. Another interesting feature in the FTIR spectrum is, unlike other bands, the vibration bands at 3420 and 1640 cm^{-1} can be assigned to the stretching and bending vibration of OH bonds, respectively [16,17]. Fig. 9 compares the FTIR absorbance spectra of α-Al_2O_3 obtained after calcination of gibbsite, boehmite or by oxidation of PM2000, and measured at room temperature. For the alumina formed on PM2000, the substrate signal was never detected in case of FTIR spectra, because the experiment was performed on the oxide scraped from the substrate.

FTIR and Raman spectroscopies both involve IR wavelength radiation and both measure the vibrational energies of molecules, but these methods rely only on different selection rules. It is possible to take literature RAMAN results as a reference to interpret our results. According to Raman results, the α-Al_2O_3 peak at 378.7 cm^{-1} can be considered as a Ref. [18], i.e. corresponding to the peak position for polycrystalline α-Al_2O_3 ceramic free from strain. Further on, the shift of Al–O vibration frequency relative to the 378.7 cm^{-1} peak position can be used to estimate intrinsic stress in samples. Since a direct relationship is expected for the 378.7 cm^{-1} band with the bending mode of oxygen atoms, the position of this peak is therefore very sensitive to the oxygen sublattice disorder resulting either from processing or non-stoichiometry. For the samples calcined at >1223 K, significant spectroscopic bands at 644 ± 4, 604 ± 5, 452 ± 3 and $382\pm4\,cm^{-1}$ appear which are identified to be the characteristic absorption bands of α-Al_2O_3 [19]. This is in good agreement with XRD observations. As mentioned previously, the frequency shift of the peak at $\sim$378.7 cm^{-1} will be attributed to the stress variation. The compressive stress in the oxide can be calculated from the frequency shift $\Delta\omega$ using the following equation:

$$\Delta\omega=\omega_{sample}-\omega_{ref}=-K\sigma \tag{4}$$

where ω_{sample} and ω_{ref} ($=378.7\,cm^{-1}$) are the peak position of the stressed and unstressed samples, σ is the intrinsic stress in GPa and K is a constant for a given compound. According to the

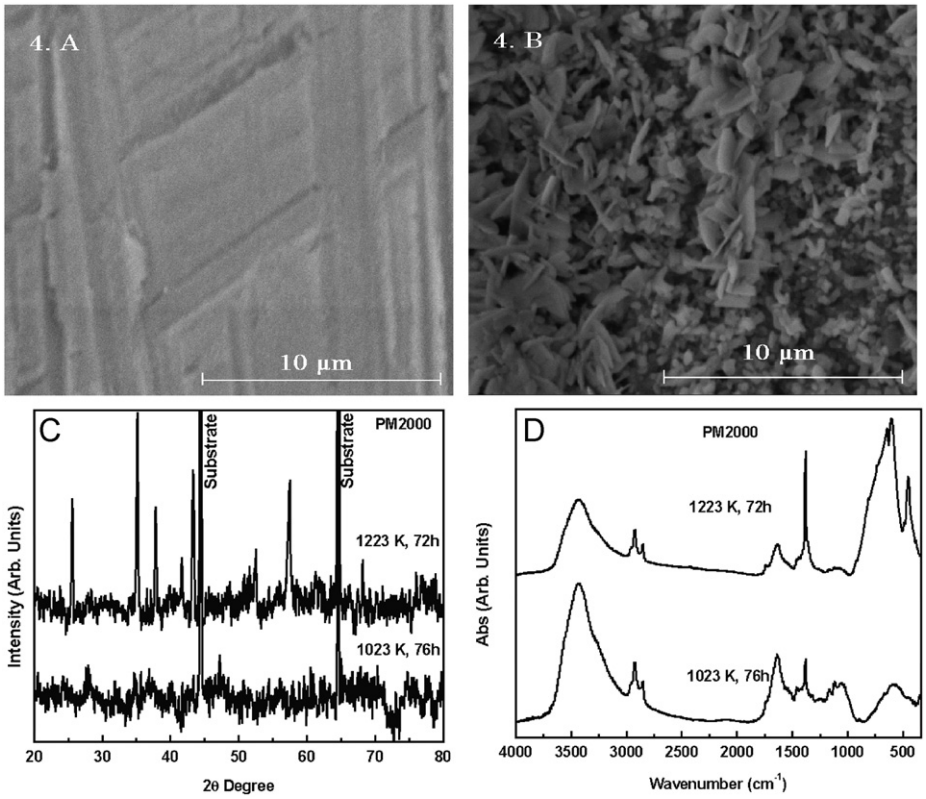

Fig. 4. SEM images of the outer oxidized surface, XRD patterns and FTIR spectra of α-Al_2O_3 obtained by oxidation of PM2000 at 1023 K for 76 h and 1223 K for 72 h.

Table 1
The average strain, stress, crystallite size and specific surface area of the α-Al_2O_3 samples obtained after calcination of gibbsite, boehmite and oxidisation of PM2000, deduced from XRD experiments except the last line whose values of intrinsic stress are deduced from FTIR experiments.

α-Al_2O_3 from	Gibbsite 1573 K, 24 h	Boehmite 1573 K, 24 h	PM2000 1223 K, 72 h
			Film adherent to the substrate
Crystallite size (D), nm	43	31	36
Strain, ε%	0.21	0.11	0.58
Stress MPa (absolute value) from XRD	3160	1700	2930
Specific surface area (S_{ssa}), m^2/g	35	48	42
Intrinsic stress (MPa) (absolute value) from IR	5330	950	Scraped film 3140

different experiments and literature, the value of K is evaluated to be 1.1 to 1.37 $cm^{-1}GPa^{-1}$ for the 378.7 cm^{-1} Raman line [18,20–22]. In the present report, K was taken as equal to 1.37 $cm^{-1}GPa^{-1}$ in order to estimate the residual intrinsic stress of our α-Al_2O_3 samples [18]. Based upon this result, the compressive intrinsic stress for all α-Al_2O_3 obtained after calcinations in this work is estimated to be on the order of 0.95–5.32 GPa.

Values are given in Table 1 and correspond to compressive stresses as in all cases the peak at 378.7 cm^{-1} is shifted towards higher values. These values are in good agreement with the literature data measured for similar materials [23–25] and the increasing stress sequence, "boehmite < PM 2000 < gibbsite", agrees that obtained by DRX. The reason which may be responsible for the compressive intrinsic stress is the lattice distortion caused by the oxygen vacancies (V_O) with different charge states. These defects are formed when the gibbsite, boehmite and aluminium were transformed into α-Al_2O_3 during the heat-treatments. Main features specific to vibration spectra of anion-nonstoichiometric α-Al_2O_3 crystals, which were due basically to changes in the effective force of interaction between vacancies and the nearest environment, were analyzed and explained by Kislov et al. [26]. The main intrinsic defects in the crystals are oxygen vacancies in different charge states: a neutral vacancy, a vacancy capturing one electron (a F^+-center) and a vacancy capturing two electrons (a F-center) [26–28]. Apart from the lattice vacancy-type defects, surface defects can also have an influence and it depends on the surface to volume ratio.

As shown in Figs. 6–8, titanium as chromium in α-Al_2O_3 lattice gives a luminescence in the visible domain. In CL, the narrow band at ~1.8 eV is attributed to chromium impurity, whereas titanium is characterized by a large band centered at ~1.7 eV [29]. By optimizing the peak position and half-width of the Gaussian peaks, it was possible to obtain a good fit for the multi-peak combination. The Gaussian peaks (dashed lines) are shown at the bottom of Figs. 6b, 7b and 8b, while the solid lines represent the linear combination of the multi-Gaussian peaks with a constant background. The peak positions are marked. Mathematic treatment of the CL spectra has shown that wide band over the interval of (2.0–6.0) eV consists of a series of overlapping bands. The main absorption bands located at about ~5.36, ~5.03, ~4.42, ~3.91

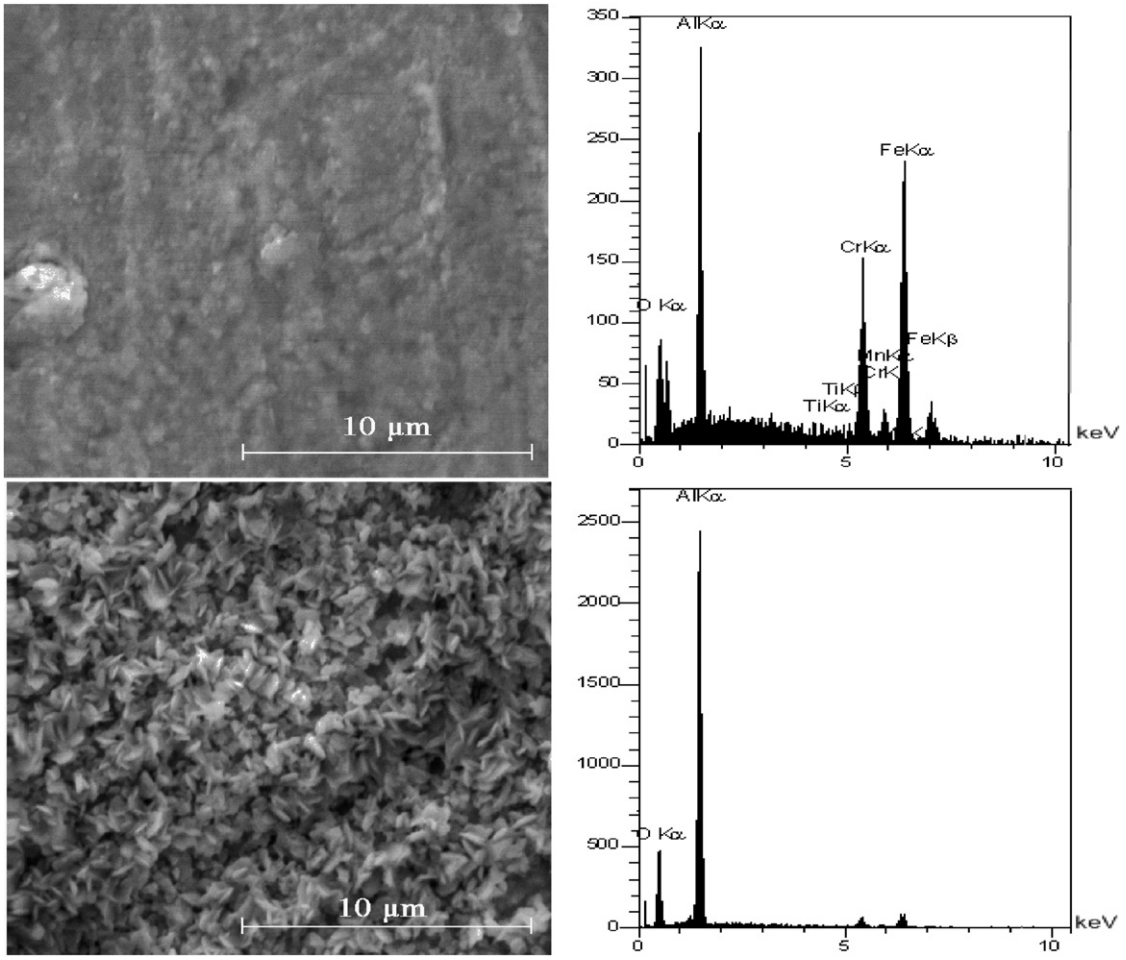

Fig. 5. SEM images of the outer surface and EDX analyses of α-Al_2O_3 films obtained by oxidation of PM2000 in air at 1023 K for 76 h (top) and 1123 K for 95 h (bottom).

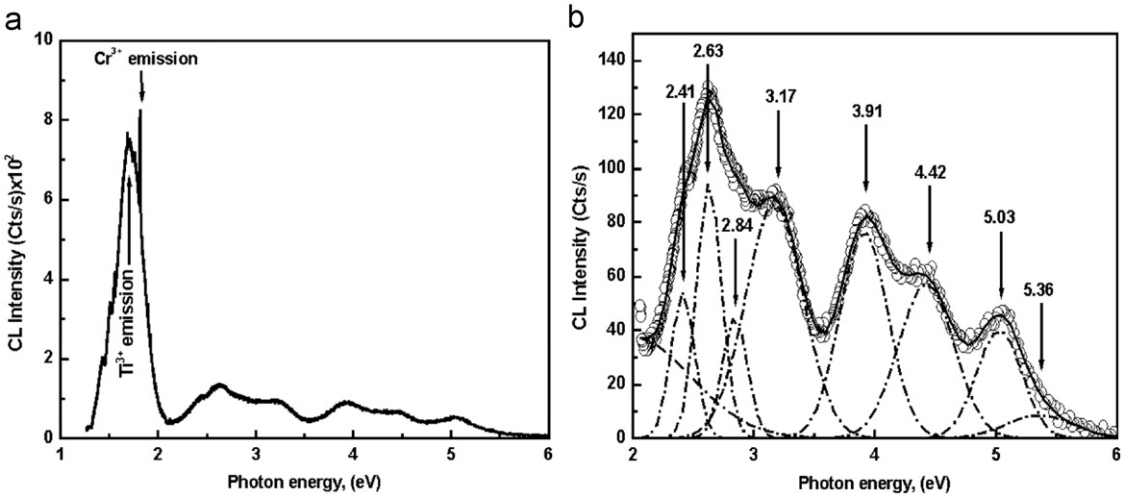

Fig. 6. Cathodoluminescence spectra of α-Al_2O_3 powder obtained by calcination of boehmite powder at 1573 K for 24 h. Gaussian deconvolution components (dashed lines) and the fit to the data (thin solid line) are shown in (b).

and ~2.42 eV occur in alpha alumina powder, and also do not change with the composition of the starting material. In Fig. 8b, the main absorption bands located at about ~5.50, ~5.03, ~4.35, ~3.88, ~3.37 and ~2.99 eV occur in α-Al_2O_3 formed from PM2000. The band at ~3.9 eV is attributed to F^+ center [29]. For instance, the CL intensity at 3.9 eV of the α-Al_2O_3 formed from gibbsite (Fig. 7b) is approximately 32 and 23 times higher than that of the α-Al_2O_3 formed from boehmite and PM2000, respectively, (Figs. 6b, 8b) measured under the same excitation conditions. Aluminas either formed by oxidation or obtained after calcination of gibbsite have greater intrinsic stresses which would correspond to a larger amount of oxygen vacancies; it can be observed that the alumina grain morphology of α-Al_2O_3 formed from gibbsite (Fig. 2) and of alumina on PM2000 (Fig. 4) looks like

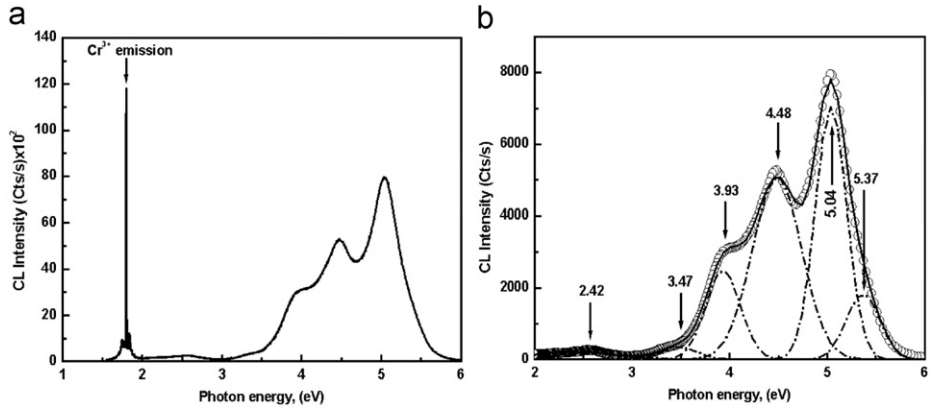

Fig. 7. Cathodoluminescence spectra of α-Al_2O_3 powder obtained by calcination of gibbsite powder at 1573 K for 24 h. Gaussian deconvolution components (dashed lines) and the fit to the data (thin solid line) are shown in (b).

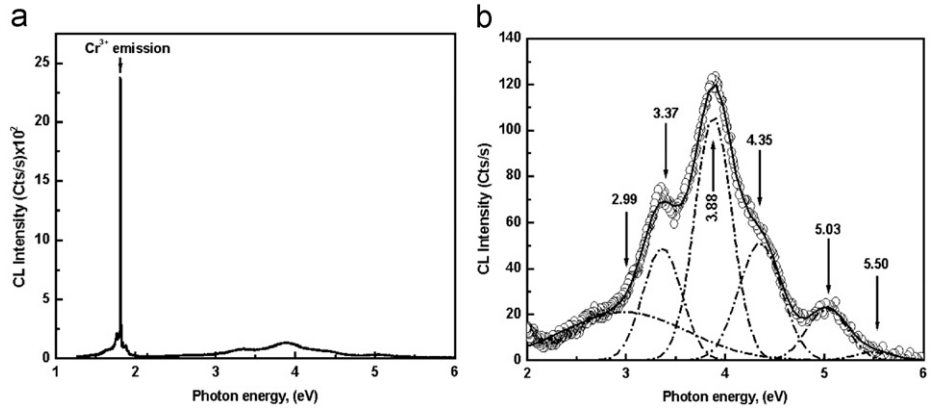

Fig. 8. Cathodoluminescence spectra of α-Al_2O_3 obtained by oxidation of PM2000 at 1223 K for 24 h. Gaussian deconvolution components (dashed lines) and the fit to the data (thin solid line) are shown in (b).

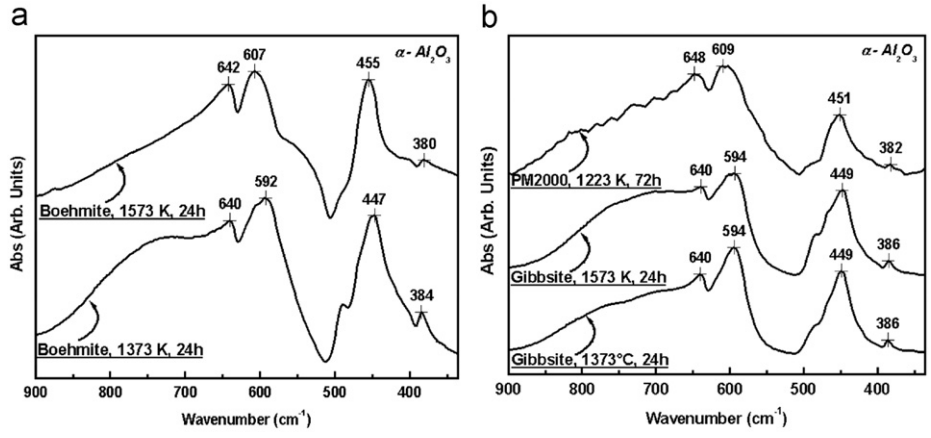

Fig. 9. Comparison of FTIR spectra of α-Al_2O_3 obtained by calcination of boehmite and gibbsite or oxidation of PM2000.

platelets or convoluted grains and differs from that of α-Al_2O_3 formed from boehmite (Fig. 1) which are spheroïdal. Such morphologies with high surface to volume ratio, like platelet morphology should favor the existence of large quantities of oxygen vacancies which induce a more distorted lattice and larger intrinsic stress [30], which testified the results of the CL spectrum (Fig. 7).

Because the α-Al_2O_3 formed from boehmite and by oxidation of PM2000 have a larger specific surface area, there exists a lot of dangling bonds in the surface. It is well known that the amount of dangling bonds and unsaturated bonds in the powder surface is heavily dependent on the crystallite size and/or on the specific surface area. The larger the crystallite size, the smaller the specific surface area, and the smaller the dangling and unsaturated bonds. This is probably the case of alpha alumina samples obtained from gibbsite for which surface effects can be neglected compared to other alumina samples (coming from boehmite or from PM2000 oxidation). Concerning alumina on PM2000, it is well known that Ti, Y, Fe, Cr "nodules" are present at the outer part of the scale [31,32], but their participation in the measurements developed in

this work is negligible as all the thickness of the film is analyzed. The better the balance between aluminium and oxygen ions according to the alumina formula, and the better the crystallization at high temperature, the smaller the defect amount due to the non-stoichiometry and the smaller the residual intrinsic stress. In the case of our samples, the more stoichiometric compound ($\sigma = -0.95$ GPa) corresponds to the α-Al_2O_3 obtained from calcinations of boehmite whose grains are regular (see Fig. 1B). Thus, it is observed in this work, that the stoichiometry of the platelet-like or convoluted grains is decreased greatly compared with that of the spherical grains. It is obvious that the particle morphology has an important influence on the phase transformation of the material, the alpha alumina particles obtained by calcination or oxidation retaining the starting material morphology as a shape memory effect.

5. Conclusions

The specific signatures of α-Al_2O_3 by Fourier transform infrared (FTIR) spectroscopy was investigated to estimate the intrinsic stress in this compound according to its elaboration mode. It allows to correlate the microstrain, determined from X-ray measurements, with the stresses determined with infrared spectroscopy and supported by cathodoluminiscence experiments. α-alumina was prepared either by calcination of boehmite or gibbsite and also generated by oxidation of a metallic FeCrAl alloy.

- XRD investigations allowed to determine the strain and the crystallite size for different α-Al_2O_3 obtained after calcination of gibbsite, boehmite or by oxidation of PM2000.
- The specific surface area of these aluminas was also evaluated and related to the alumina morphology observed by SEM.
- The infrared peak at 378.7 cm^{-1} was used as a reference for stress free α-alumina and the shift of this peak allowed to estimate intrinsic stresses whose evolution according to the elaboration mode is similar to that of stresses determined by XRD. Intrinsic stresses were related to the morphology and to the specific surface area of aluminas according to their elaboration mode.
- Aluminas either formed by oxidation or obtained after calcination of gibbsite have greater intrinsic stresses which would correspond to a larger amount of oxygen vacancies than in alumina formed by calcination of boehmite. The difference in oxygen vacancies amount between gibbsite and boehmite was confirmed by cathodoluminescence spectra for which peak intensity gives information on the defects.
- It is suggested that this is related to the platelet morphology of aluminas issued from gibbsite or PM2000 oxidation, the alpha alumina particles retaining the starting material morphology as a shape memory effect.

References

[1] A.M. Huntz, P.Y. Hou, R. Molins, Mater. Sci. Eng. A 467 (2007) 59–70.
[2] L. Maréchal, B. Lesage, A.M. Huntz, R. Molins, Mater. High Temp. 20 (2003) 295–301.
[3] W.F. Zhang, Y.L. He, M.S. Zhang, Z. Yin, Q. Chen, J. Phys. D 33 (2000) 912–916.
[4] J.W. Ager III, D.K. Veirs, G.M. Rosenblatt, Phys. Rev. B 43 (1991) 6491–6499.
[5] B. Li, D. Yu, S.-L. Zhang, Phys. Rev. B 59 (1999) 1645–1648.
[6] A. Boumaza, L. Favaro, J. Lédion, G. Sattonnay, J.B. Brubach, P. Berthet, A.M. Huntz, P. Roy, R. Tétot, J. Solid State Chem. , doi:10.1016/j.jssc.2009.02.006.
[7] B.D. Cullity, Elements of X-ray Diffraction, Addison-Wesley, Reading, MA, 1972 350.
[8] T. Tsuchida, K. Horigome, Thermochim. Acta 254 (1995) 359–370.
[9] K.J.D. MacKenzie, J. Temuujin, M.E. Smith, P. Angerer, Y. Kameshima, Thermochim. Acta 359 (2000) 87–94.
[10] K.J.D. MacKenzie, J. Temuujin, K. Okada, Thermochim. Acta 327 (1999) 103–108.
[11] N.B. Pilling, R.E. Bedworth, J. Inst. Met. 29 (1923) 529–582.
[12] A.M. Huntz, L. Maréchal, B. Lesage, R. Molins, Appl. Surf. Sci. 252 (2006) 7781–7787.
[13] S.J. Gregg, K.S.W. Sing, Adsorption, Surface Area and Porosity, second ed., Academic Press, London, 1982.
[14] I. Levin, D. Brandon, J. Am. Ceram. Soc. 81 (8) (1998) 1995–2012.
[15] P.A. Dokhale, N.D. Sali, P. Madhu Kumar, S.V. Bhoraskar, V.K. Rohatgi, V.N. Bhoraskar, S.K. Date, S. Badrinarayanan, Mater. Sci. Eng. B 49 (1997) 18–26.
[16] C. Morterra, G. Magnacca, Catal. Today 27 (1996) 497–532.
[17] C. Ma, Y. Chang, W. Ye, W. Shang, C. Wang, J. Colloid Interface Sci. 317 (2008) 148–154.
[18] G.H. Watson, W.B. Daniels, C.S. Wang, J. Appl. Phys. 52 (1981) 956–958.
[19] A.S. Barker Jr., Phys. Rev. 132 (1963) 1474–1481.
[20] J.-A. Xu, E. Huang, J.-F. Lin, L.Y. Xu, Am. Mineralogist 80 (1995) 1157–1165.
[21] S.P.S. Porto, R.S. Krishnan, J. Chem. Phys. 47 (1967) 1009–1012.
[22] S. Shin, F.H. Pollak, P.M. Raccah, Effects of uniaxial stress on the Raman frequencies of Ti_2O_3 and Al_2O_3, in: M. Balkanski, R.C.C. Leite, S.P.S. Porto (Eds.), Proceedings of the third international conference on light scattering in solids, Wiley, New York, 1976, pp. 401–405.
[23] V.K. Tolpygo, J.R. Dryden, D.R. Clarke, Acta Mater 46 (1998) 927–937.
[24] H. Echsler, E. Alija Martinez, L. Singheiser, W.J. Quadakkers, Mater. Sci. Eng. A 384 (2004) 1–11.
[25] V.K. Tolpygo, D.R. Clarke, Surf. Coat. Technol. 120–121 (1999) 1–7.
[26] A.N. Kislov, V.G. Mazurenko, K.N. Korzov, V.S. Kortov, Physica B 352 (2004) 172–178.
[27] S. Michizono, Y. Saito, Suharyanto, Y. Yamano, S. Kobayashi, Vacuum 81 (2007) 762–765.
[28] Z.Q. Yu, C. Li, N. Zhang, J. Lumin. 99 (2002) 29–34.
[29] M. Ghamnia, C. Jardin, M. Bouslama, J. Electron Spectrosc. Relat. Phenom. 133 (2003) 55–63.
[30] K. Bouzid, A. Djelloul, N. Bouzid, J. Bougdira, Phys. Status Solidi (a) 206 (2009) 106–115.
[31] L. Maréchal, B. Lesage, A.M. Huntz, R. Molins, Oxid. Met. 60 (2003) 1–28.
[32] M. Berlanga, J.L. González-Carrasco, M.A. Montealegre, M.A. Muñoz-Morris, Intermetallics 12 (2004) 205–212.